State Analyses of Metal Ions in Flux†

Nobuya IWAMOTO*, Yukio MAKINO and Kazumi OGINO*****

Abstract

To determine the state of cation in molten flux, the various means, such as emission X-ray peak shift, optical absorption and ESCA, were applied. Also, the structural change on rapid quenching from the molten state was studied by means of X-ray small angle scattering and electron microscopy.

Introduction

The flux in welding technology plays an important role. It prevents surface oxidation, removes non-metallic inclusions and refines materials. The choice of flux, however, is still determined by the experienced manufacture. Consequently a fundamental understanding is necessary concerning the variation of physical properties, such as surface tension, viscosity and so on, as a function of temperature and composition.

Many unknowns exist as to the effect of oxide or fluoride addition on the properties of flux. Even though they will be cleared in future, the behaviors of cations and anions in the molten state should be explained at this time.

Different kinds of spectroscopy have been developed for investigating the electronic structure of material. The most well-known are optical, infrared and ultraviolet spectroscopy.

X-ray emission and absorption spectroscopy, nuclear resonance spectroscopy (NMR), electron spin resonance spectroscopy (ESR) and Mössbauer resonance spectroscopy are also well known. ESCA (Electron Spectroscopy of Chemical Analysis) has been recently developed with higher resolution.

When electron beam, X-ray and charged particle strike a substance, X-ray and/or electron will be ejected. From the measurement of high accuracy and resolving power, a slight chemical shift of the specimen has been easily detected.

In this paper, the authors have given considerations to the fundamental means to do state analysis of cations in molten flux.

Experimental Procedures

The systems, $Na\,O-Al_2O_3-SiO_2$, $CaO-Al_2O_3-SiO_2$ and $CaO-Cr_2O_3-SiO_2$ and $PbO-SiO_2$ were studied. Molten slag at a temperature 100℃ higher than the melting point kept at that level for 1 hr was quenched into ice-cooled mercury. For the identification of small crystallites, an X-ray small angle scattering study was used. The experimental conditions was as follows:

Target: Cu (Ni filtered)

Exc. Condn.: 50 kV×30 mA

Detector: Scintilation counter

The back reflection method was applied by using rays covered from visible to near-infrared regions. The apparatus used was a spectrometer of EPS—3T (Hitachi Co. Ltd.). Specimen used are summarized in **Table 1.**

For the measurement of magnetic property, the Faraday method was used in the temperature ranges from liquid N_2 up to room temperature.

For comparison, magnesium chromite that have various compositions ($N_{Cr}/N_{Cr}+N_{Mg}$) was measured.

The study of emission X-ray peak shift was carried out with a fluorescent X-ray spectrometer of GF—S (Rigaku Denki Co. Ltd.). The experimental conditions was as follows:

Target: W

Exc. Condn.: 50 kV×50 mA

Table 1. The notation of specimens in the system Cr_2O_3—CaO—SiO_2.

CaO/SiO_2 / H_2/CO_2		30/70	35/65	40/60	45/55	50/50	55/45
1 wt% Cr_2O_3	15		15CR1-65	15CR1-60	15CR1-55	15CR1-50	15CR1-45
	5		5CR1-65	5CR1-60	5CR1-55	5CR1-50	5CR1-45
	1		1CR1-65	1CR1-60	1CR1-55	1CR1-50	1CR1-45
	in air	CR1-70	CR1-65	CR1-60	CR1-55	CR1-50	CR1-45
3 wt% Cr_2O_3	15		15CR3-65	15CR3-60	15CR3-55	15CR3-50	15CR3-45
	in air	CR3-70	CR3-65	CR3-60	CR3-55	CR3-50	CR3-45
50 wt% CaO	in air	5 wt% Cr_2O_3	10 wt% Cr_2O_3	15 wt% Cr_2O_3	20 wt% Cr_2O_3	25 wt% Cr_2O_3	
		C50-5CR	C50-10CR	C50-15CR	C50-20CR	C50-25CR	

† Received on May 10, 1972

* Professor

** Hitachi Co. Ltd., Semiconductor & Integrated Circuits div. (Formerly Graduate Student at Osaka University)

*** Professor, Dep.of Metallurgy, Faculty of Engineering, Osaka University

Crystal: EDDT or Topaz
Detector: Gas-flow proportional counter or Scintilation counter.

The experiment of electron microscopy was performed with HU—11 ES (Hitachi Co.Ltd.).

Experimental Results and Discussions

It is important in investigating the structure of flux to consider whether the molten structure could be brought to room temperature without change of it's structure. Even if an amorphous pattern of X-ray diffraction was shown, it would be impossible to conclude that nucleation and crystal growth did not occur[1]. The matrix composition was not the same as the oridinal one if existing many crystallites were observed by the X-ray small angle scattering method. All specimens covering all the regions of the system CaO —Al_2O_3—SiO_2 have shown the appearences of small crystallites varying size from several hundred to thirty Å. Two examples are given in **Table 2.**

To study the absorption spectrum of transition metal ions in flux, or to estimate the transition metal ions from their optical absorption, the individual extinctions with different valence states have to be determined. Transition metals when introduced in a molten flux, very often demonstrate to have more than one oxidation state-each of which gives rise to characteristic absorption of radiation. According to crystal field theory, the calculated value of optical transition will be compared with the one obtained experimentally in the simple structure[2]. In this paper, the system CaO—Cr_2O_3—SiO_2 will be briefly described.

When the symmetry is cubic, a fivefold degenerate D state splits into two states, a triply-degenerate state and a double-degenerate state. Correspondingly, the sevenfold degenerate F state splits into two triply degenerates and one nondegenerate state. Term splitting in fields of cubic symmetry are shown in **Fig. 1.**

These diagrams enable us to understand under what circumstances one may infer something about stereochemistry from the number of unpaired electrons since it is clear that the symmetry as well as the strength of the ligand field effects electron pairing.

Only the splitting of the ^4F ground term of the free Cr^{3+} ion in a ligand field of symmetry O_h has been considered until now. The appearance of both observed long wave-length chromium bands ($^4A_{2g} \rightarrow {}^4T_{2g}$, $^4A_{2g} \rightarrow {}^4T_{1g}$) could be explained.

Table 2. Small angle scattering results

Specimens	Radius (Å)
$CaO–Al_2O_3–SiO_2$	
30–20–50	384～62
16–34–50	394～37

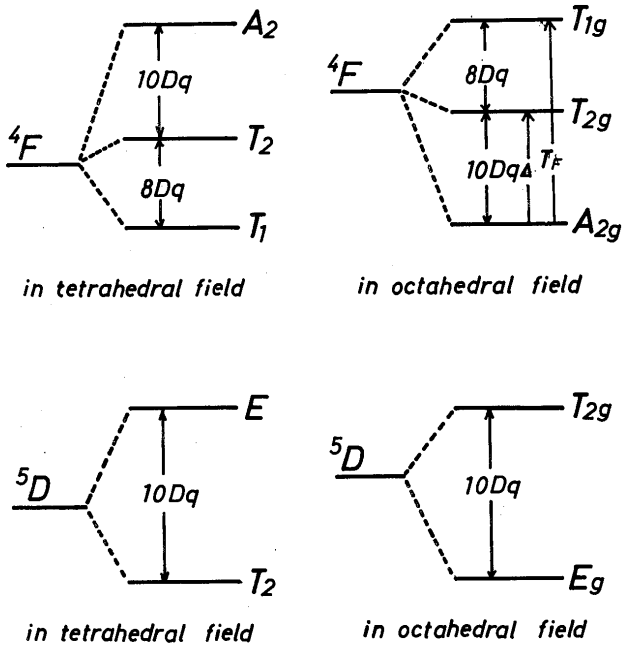

Fig. 1. Splitting of F and D terms in octahedral and tetrahedral fields.

Visible absorption results of various standard specimens having chromium are shown in **Fig. 2.** A significant fact is that the standard specimen in aqueous solution indicates different absorption behavior.

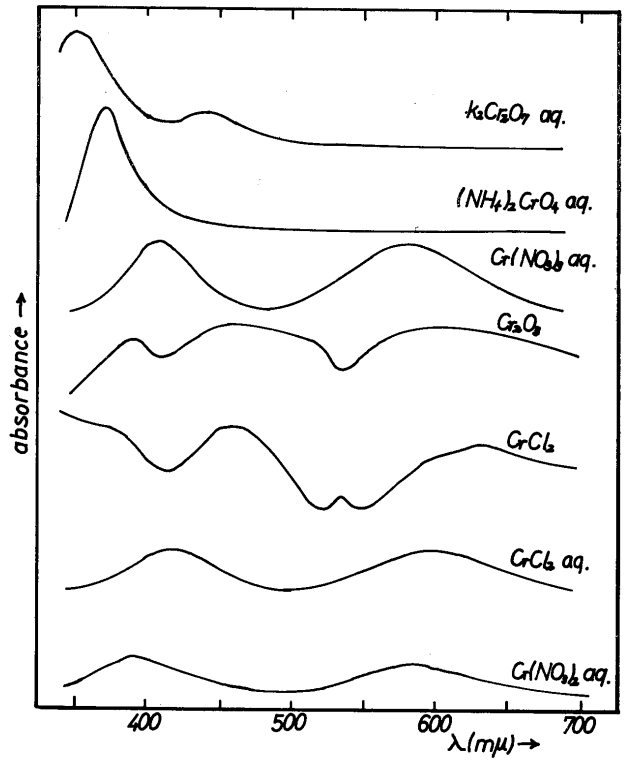

Fig. 2. Visible absorption results of various standard specimens.

Figs. 3 (a) and **3** (b) give the absorption results of CR1 and C50 series. It would be seen that the band near 600 mμ disappear in the latter.

Secondary, the absorption results of the strongly reduced specimens are shown in **Fig. 4 (a).** For comparison, the result of the solution treated by hydrochloric acid are shown in **Fig. 4 (b).**

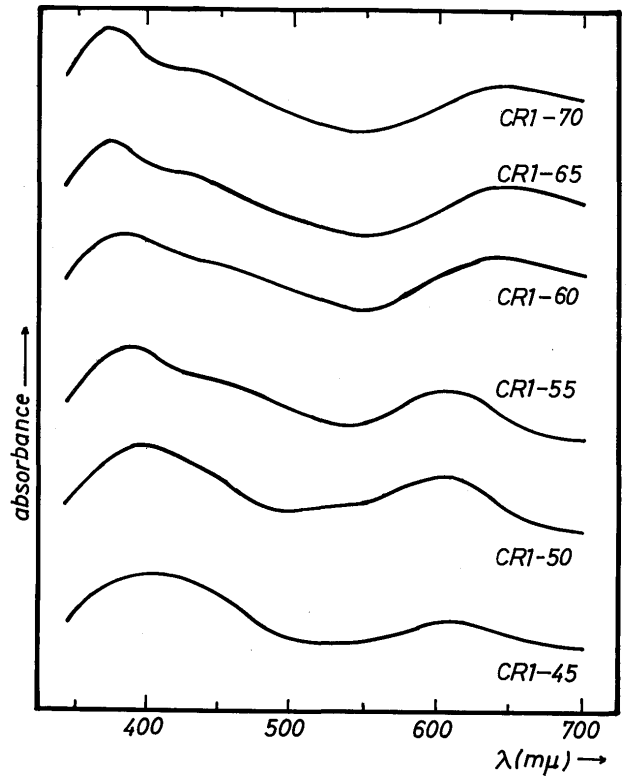

Fig. 3 (a). Visible absorption results (CR1 series).

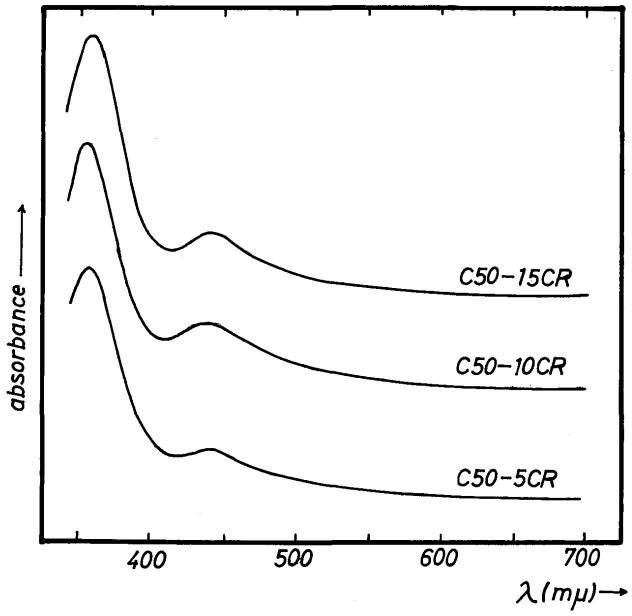

Fig. 3 (b). Visible absorption results (C50 series).

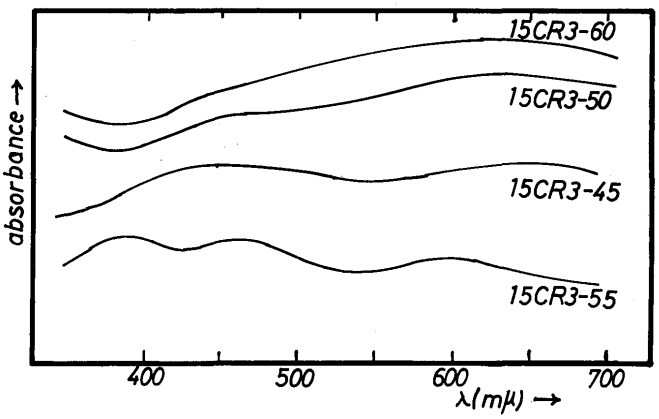

Fig. 4 (a). Visible absorption results (15CR3 series).

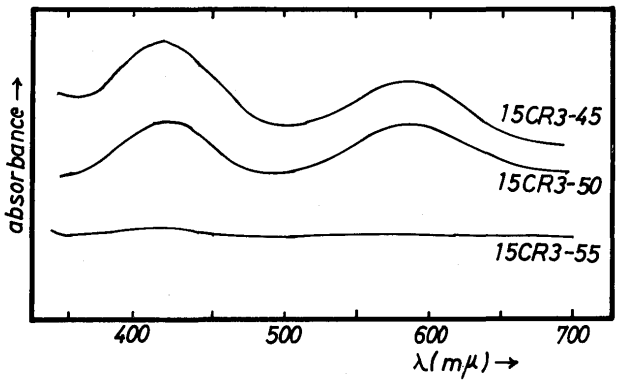

Fig. 4 (b). Visible absorption results of 15CR3 series specimens dissolved with 3N-Hcl aq.

It is clear from these results that notable difference occur when the specimens were dissolved by acid in the absorption behavior. With lowering oxygen partial pressure in the equilibrating atmosphere and increasing SiO_2 content in flux, the extinction become more dull and leaves only peak nere 630 mμ. When the inverse conditions holds, there appears peak near 450 mμ.

The state diagram of chromium ion by visible absorption spectra is shown in **Fig. 5.** It will be antici-

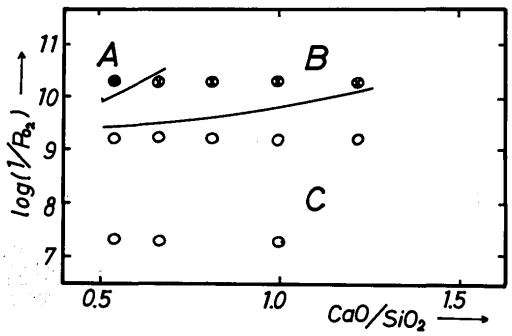

Fig. 5. The state diagram of chromium ion by visible absorption spectra
A: Absorption band exists near 600 mμ.
B: Absorption band exists near 450 mμ and 600 mμ.
C: Absorption band exists near 450 mμ.

pitated that there are three groups classified with the experimental conditions, the equilibrated oxygen partial pressure and the basicity.

Tanabe and Sugano[3] gave the Racah parameter B, which gires a measure of the interelectronic repulsion energies. The Racah parameter may be evaluated explicitly from Eq. (1).

$$B=1/3\cdot(2\Delta-T_F)(T_F-\Delta)/(9\Delta-5T_F) \quad (1)$$

This expression is valid for the $^4A_{2g}\rightarrow{}^4T_{1g}$ transition denoted by T_F and for the $^4A_{2g}\rightarrow{}^4T_{2g}$ transition by Δ. The point charge and point dipole approximation of crystal field theory assume that the Racah parameter is invarient under a simple lattice expansion or contraction, and some of the solid solution series do indeed exhibit this invariance[4]. However, it was found that ruby and very low chromia content spinel display anomalous behavior in this respect[5].

We now wish to see whether we can account for the structure of slag from the interrelation between the Racah parameter and the basicity.

In **Fig. 6,** the calculated value by Eq. (1) are plotted against the CaO/SiO_2 values. The points do in fact lie fairly close to the parabola.

In despite of the amorphous structure that the nearest-neighbor ordering is only preserved in slag, there seem to exist some regularity as if they behave like crystalline state. Likewise, the relationship between the Racah parameter and Δ are shown in **Fig. 7.**

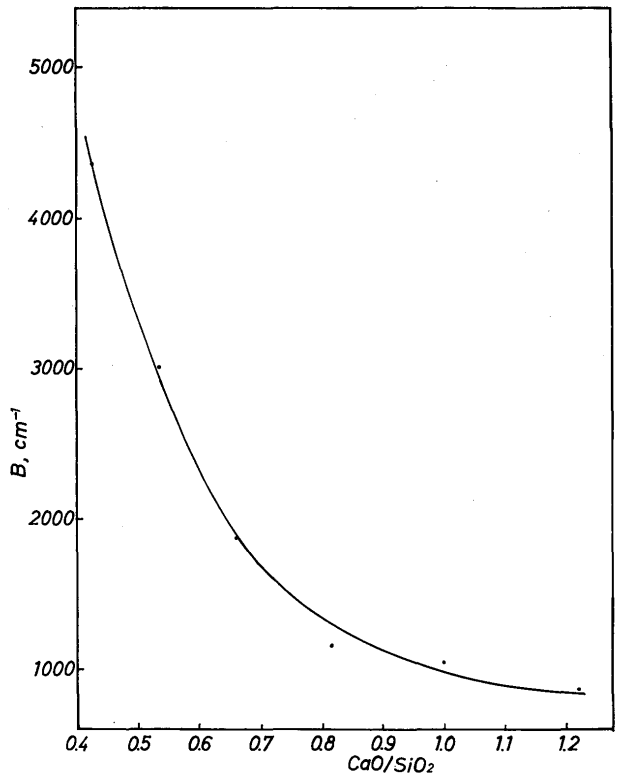

Fig. 6. Relationship between the Racah parameter B and the basicity.

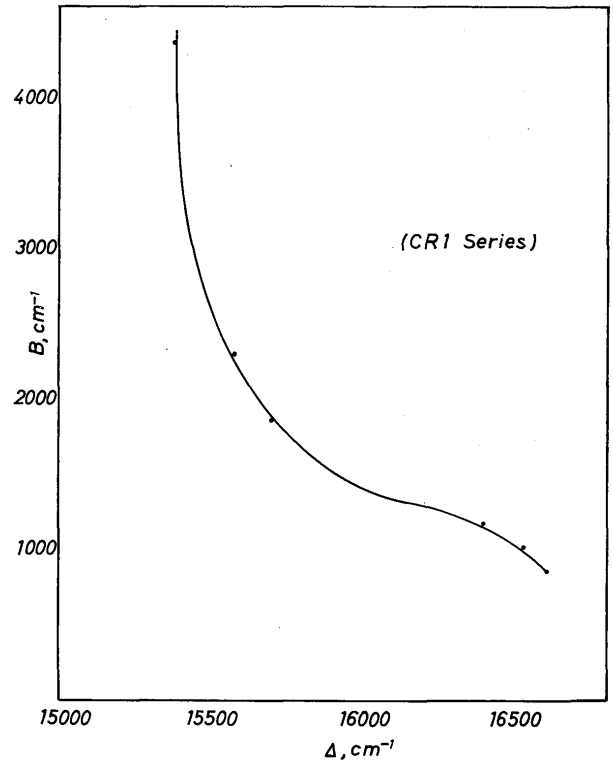

Fig. 7. Relationship between the Racah parameter B and the Δ.

The information of magnetic property gives insight as for valency of cation in crystal. The results obtained are shown in **Figs. 8** and **9.**

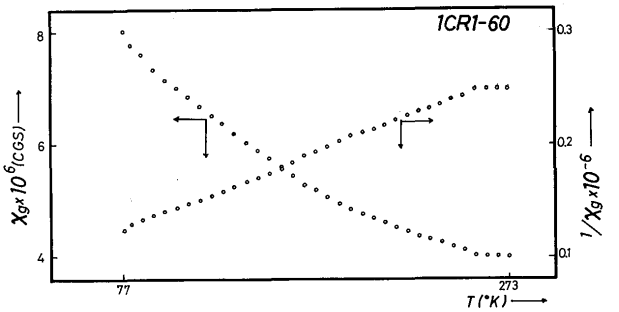

Fig. 8. The variation of magnetic susceptibility with temperature (1CR1-60).

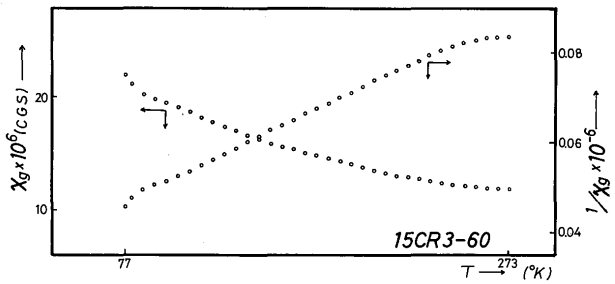

Fig. 9. The variation of magnetic susceptibility with temperature (15CR3--60).

It will be seen that they show paramagnetic behavior and do not have transition point within the range in the present experiment.

For comparison, magnesium chromite which was assigned to have Cr^{2+} state[6] was measured.

For the calculation of effective magnetic moment, the following equations[6] were used.

$$\chi_A = N\beta^2\mu_{eff}^2 / 3k(T-\Theta) \quad (2)$$

N: Avogadro's number
β: Bohr magneton
k: Boltmann constant
T: Absolute temperature
Θ: Weiss constant

$$\mu_{eff}^2 = C_{Cr}{}^{2+}(\sqrt{n(n+2)})^2 + C_{Cr}{}^{3+}(\sqrt{n'(n'+2)})^2 \quad (3)$$

C_{Cr}^{2+}, C_{Cr}^{3+}: The number of chromium ions per molecule
n, n' : The number of unpaired electrons in Cr^{2+} and Cr^{3+}

Electronic configurations of d^4 are shown in **Fig.10.**

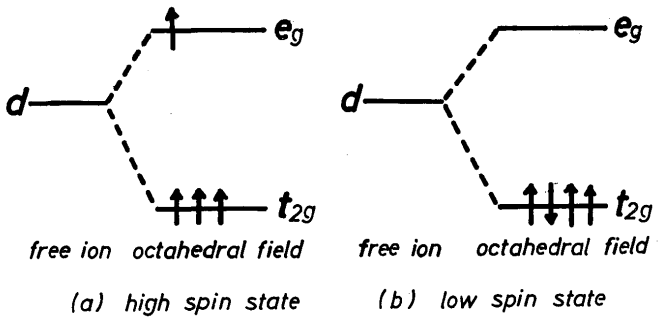

Fig. 10. Electronic configurations of d^4.

In **Table. 3,** the effective magnetic moments of magnesium chromite and slags are given. The values in parenthesis are the calculated one as high spin state and spin only. With regard to this calculation, it should be pointed out that it is impossible to get good agreement and that the values in slag are extraordinaliily high. It should be taken some angular momentum contribution into consideration. It was impossible to detect the valency change of chromium ion in slag from the magnetic measurement.

The emission X-ray peak shift values are summarized in **Table 4.** It is anticipitated that a strongly

Table 3. Effective magnetic moment (μ_{eff}) of 1CR1--60, 15CR3--60 and $MgCr_2O_4$.

Material	μ_{eff}	Molecular Formula
$MgCr_2O_4$ (k=2/3 r=30)	5.85 (5.48)	$MgO \cdot Cr_2O_3$
$MgCr_2O_4$ (k=3/4 r=30)	6.68 (6.48)	$(MgO)_{0.75}(Cr\,O)_{0.25}(Cr_2O_3)$
$MgCr_2O_4$ (k=3/4 r=100)	7.90 (6.48)	$(MgO)_{0.75}(CrO)_{0.25}(Cr_2O_3)$
1CR1-60	5.81	$(Cr_2O_3)_{0.004}(CaO)_{0.415}(SiO_2)_{0.581}$
15CR3-60	6.18	$(Cr_2O_3)_{0.012}(CaO)_{0.411}(SiO_2)_{0.577}$

Table 4. Emission X-ray peak shift values $\Delta^\circ(2\theta)$.

Specimens	$\Delta^\circ(2\theta)$
Cr (metal)	—
Cr (power)	—
Cr_2O_3	−0.010
$K_2Cr_2O_7$	+0.017
1CR1–50	−0.013
1CR1–65	−0.014
15CR1–50	−0.017
15CR1–65	−0.020
iron chromite[7]	−0.048

reduced chromium ion has a tendency to show much peak shift. However, it may be clear that the amount of shift is less than in iron chromite with Cr^{2+} state which was investigated with various means such as Mössbauer resonance, thermogravimetric, specific gravity and so on[7]. From the results obtained, it seems to be difficult to accept the previous opinion that the state of chromium in the system $CaO—SiO_2$ is probably divalent from the observation of the color change[8].

By the study of electron microscopy, the precipitates were observed in the systems $CaO—Al_2O_3—SiO_2$ and $Na_2O—Al_2O_3—SiO_2$. The results were shown in **Photos. 1** and **2.**

Lastly, the results of ESCA at the composition of $4PbO—SiO_2$ and shown in **Fig. 11.** The summarized studies should be done in future.

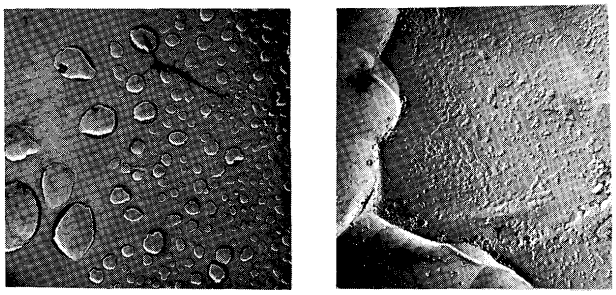

Photo. 1. Electron micrographs (×12,000).

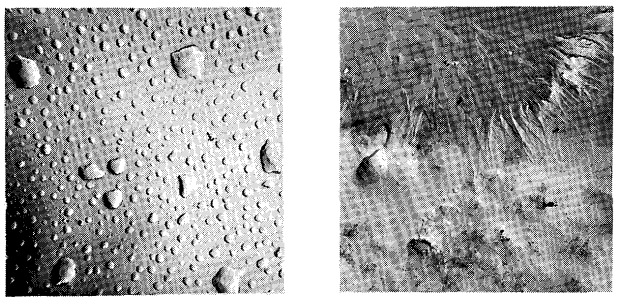

(×16,000). (×12,000)

Photo. 2 Electron micrographs

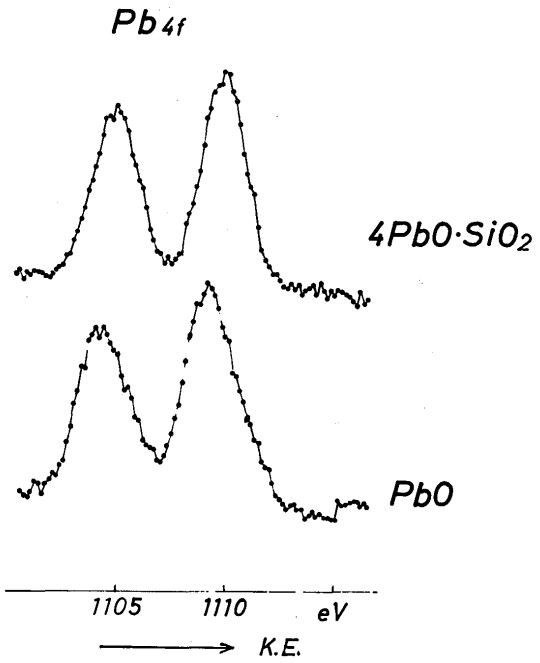

Fig. 11 (a). Results of ESCA.

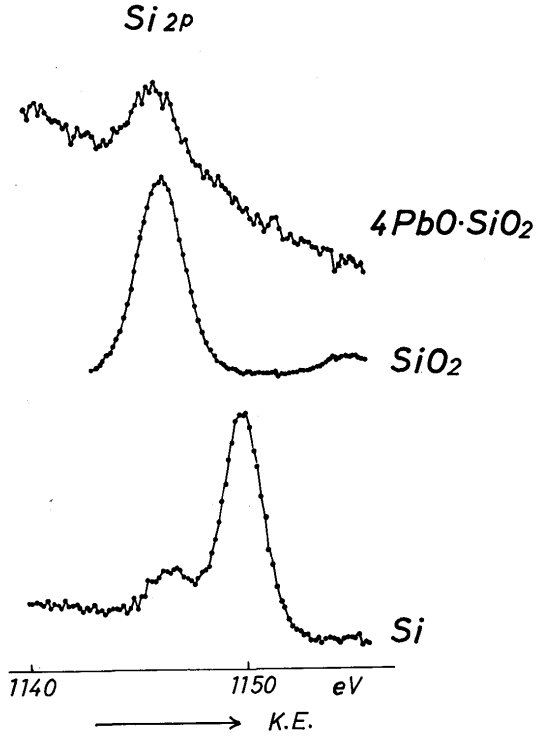

Fig. 11 (b). Results of ESCA.

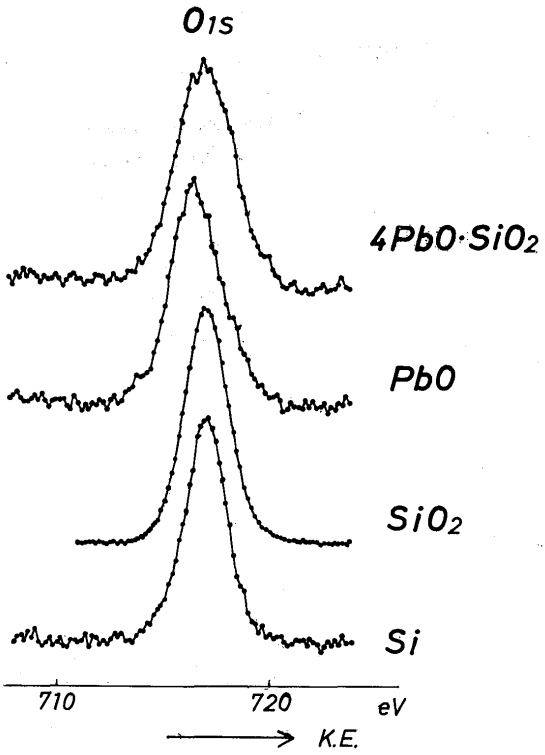

Fig. 11 (a). Results of ESCA.

Conclutions

There are many questionable conclusions as to the valence change of cations in flux. Until now, only limited means were applied to derive the conclusions. In the future, all-around studies should be done.

References

1) N. Iwamoto, Y. Makino, I. Satou and K. Ogino : *Technol. Repts. Osaka Univ.*, **21** (1971), p. 113.
2) H. L. Schläfer and G. Gliemann. Basic Principles of Ligand Field Theory" Wiley-Interscience, N. Y. (1969).
3) Y. Tanabe and S. Sugano : *J. Phys. Soc. Japan*, **9** (1954), p. 753, 766.
4) C. P. Pool Jr. : *J. Phys. Chem. Solids*, **25** (1964), p. 1169.
5) J. Graham and D. E. Scaife : *Nature*, **192** (1961), p. 161.
6) C. Greskovich and V. S. Stubican : *J. Phys. Chem. Solids*, **27** (1966), p. 1379.
7) N. Iwamoto and A. Adachi : *Trans. ISIJ*, **9** (1969), p. 59.
8) F. Körber und W. Oelsen : *Mitt. K. W. Inst. Eisenforg.*, **179** (1935), p. 231.